

## Phytotoxic $\beta$ -resorcylic acid derivatives from the endophytic fungus *Lasiodiplodia theobromae* in the mangrove plant

Yoshihito Shiono<sup>a,\*</sup>, Shiho Sato<sup>a</sup>, Ferry Ferdiansyah Sofian<sup>a</sup>, Takuya Koseki<sup>a</sup>,  
Fajar Fauzi Abdullah<sup>b</sup>, Supriatno Salam<sup>c,d</sup>, Desi Harneti<sup>c</sup>, Rani Maharani<sup>c</sup>, Unang Supratman<sup>c</sup>

<sup>a</sup> Department of Food, Life, and Environmental Science, Faculty of Agriculture, Yamagata University, Tsuruoka, Yamagata, 997-8555, Japan

<sup>b</sup> Department of Chemistry, Faculty of Mathematics and Natural Sciences, Universitas Garut, Garut, 44151, Indonesia

<sup>c</sup> Department of Chemistry, Faculty of Mathematics and Natural Sciences, Universitas Padjadjaran, Jatinangor, 45363, Indonesia

<sup>d</sup> Faculty of Pharmacy, Universitas Mulawarman, Samarinda 75123, Kalimantan Timur, Indonesia

### ARTICLE INFO

#### Keywords:

$\beta$ -resorcylic acid derivatives  
*Lasiodiplodia theobromae*  
Phytotoxicity  
*Digitaria ciliaris*  
*Lactuca sativa*

### ABSTRACT

Three new  $\beta$ -resorcylic acid derivatives, 1–3, were obtained from the endophytic strain *Lasiodiplodia theobromae* GI-1005, which was isolated from the mangrove plant *Rhizophora mucronata*. The structures of new compounds together with five known compounds were elucidated by NMR and MS analyses, and chemical means. The isolated compounds were evaluated for phytotoxicity against *Digitaria ciliaris* (southern crabgrass) and *Lactuca sativa* (lettuce). Compound 1 showed growth inhibitory effects against *D. ciliaris* in a dose-dependent manner.

### 1. Introduction

Endophytic fungi inhabit healthy plant tissues and do not cause noticeable symptoms of infection or disease. They can benefit the host in a number of ways, such as producing bioactive secondary metabolites, promoting germination and shoot development, inducing growth, and facilitating the ability of host plants to tolerate biotic or abiotic stress (Hiruma et al., 2018). Endophytes interact closely with the host plant, and metabolites produced by endophytes can protect plants from adverse environmental changes (Bastias et al., 2017). Endophytes are important new resources of natural bioactive compounds with potential impacts on agriculture, medicine, and food industries (Segaran and Sathivelu, 2019). Bioactive compounds isolated from endophytic fungi, such as alkaloids, terpenoids, steroids, quinones, lignans, phenols, and lactones, some of which are widely used in pharmacy (Martinez-Klimova et al., 2017).

In our previous studies on mangrove plants, we discovered several secondary metabolites with phytotoxic effects, including  $\beta$ -resorcylic acid derivatives from *L. theobromae* GC-22 isolated from the mangrove plant *Xylocarpus granatum* (Sato et al., 2021).

The present work was performed within the scope of chemical screening programs and led to the isolation of the fungus *L. theobromae* GI-1005 from the inner bark of the mangrove plant *Rhizophora mucronata*, which grows on the coastline of Santolo beach in Indonesia.

We report the isolation, structural determination, and biological activities of three new  $\beta$ -resorcylic acid derivatives (1–3) from methanol extract of *L. theobromae* culture.

Compound 1 was obtained as a white, amorphous solid, and was determined to have the molecular formula of  $C_{17}H_{24}O_5$  using a combination of HRESITOFMS and  $^{13}C$  NMR data, which indicated six degrees of unsaturation. UV spectrum, with absorption maxima at 265 and 302 nm, indicated the presence of a conjugated chromophore, and IR spectrum, with absorption bands at 3316 and 1643  $cm^{-1}$ , suggested the presence of OH and  $\alpha,\beta$ -unsaturated lactone carbonyl groups. The  $^1H$  and  $^{13}C$  NMR data (Table 1), combined with HSQC spectrum, displayed signals for a secondary methyl [ $\delta_H$  1.34 (3H, d,  $J = 6.2$  Hz, Me-17);  $\delta_C$  21.6 (C-17)], a methoxy [ $\delta_H$  3.74 (3H, s, Me-18),  $\delta_C$  55.4 (C-18)], six methylenes [ $\delta_H$  1.44–1.84 (H-4, 5, 6) 1.25–1.32 (m, H-8), 1.91–2.10 (m, H-8), 1.47–1.84 (m, H-9), 2.13–2.20 (m, H-10), and 3.63–3.71 (m, H-10)], two oxygenated methines [ $\delta_H$  5.09–5.16 (m, H-3), 3.89–3.96 (m, H-7);  $\delta_C$  75.2 (C-3), 68.2 (C-7)], one tetra-substituted benzene ring [ $\delta_H$  6.27 (1H, d,  $J = 2.7$  Hz, H-12), 6.32 (1H, d,  $J = 2.7$  Hz, H-14);  $\delta_C$  148.5 (C-11), 110.9 (C-12), 163.9 (C-13), 98.9 (C-14), 166.1 (C-15), 104.8 (C-16)], and one ester carbonyl [ $\delta_C$  171.9 (C-1)] group. Analysis of the  $^1H$ - $^1H$  COSY spectrum revealed structural fragments from C-3 to C-10 and C-3 to C-17 (Fig. 2). The HMBC analysis of H-3 to C-1, H-10 to C-12, and C-16 indicated that the benzene moiety was fused with a 12-membered resorcylic acid lactone ring (Fig. 1). To de-

\* Corresponding author.

E-mail address: [yshiono@tds1.tr.yamagata-u.ac.jp](mailto:yshiono@tds1.tr.yamagata-u.ac.jp) (Y. Shiono).

**Table 1**  
 $^{13}\text{C}$ -NMR NMR Data (150 MHz,  $\text{CDCl}_3$ ) for Compounds 1–3.

No.	1	2	3
1	171.9 s	170.9 s	171.7 s
3	75.2 d	72.2 d	73.1 d
4	30.9 t	32.7 t	31.4 t
5	23.5 t	17.6 t	40.2 t
6	34.8 t	37.3 t	211.9 s
7	68.2 d	70.9 d	38.1 t
8	29.8 t	38.3 t	22.1 t
9	30.9 t	125.9 d	30.9 t
10	33.8 t	136.7 d	34.3 t
11	148.5 s	143.9 s	148.8 s
12	110.9 d	107.9 d	110.6 d
13	163.9 s	164.2 s	160.6 s
14	98.9 d	99.8 d	101.7 d
15	166.1 s	164.7 s	165.8 s
16	104.8 s	104.7 s	105.1 s
17	21.6 q	19.9 q	19.2 q
18	55.4 q	55.5 q	

termine the configuration at C-7, the secondary alcohol was converted into the (*S*)- and (*R*)-MTPA esters (**1a** and **1b**). Based on the  $\Delta\delta$  ( $\delta_S - \delta_R$ ) values of both MTPA esters (Fig. 3), the configuration of C-7 was determined to be *R*. In addition, the absolute configuration of **1** was elucidated by comparing its experimental electronic circular dichroism (ECD) spectrum with the ECD spectra calculated for isomers of **1** (Fig. 4). The results showed that the theoretical ECD data for the (*3S,7R*)-isomer of **1** was in good agreement with the experimental spectrum. Finally, the absolute configuration of **1** was assigned to (*3S,7R*)-7-hydroxy-13-*O*-methyl-*de*-*O*-methylsiasiodiplodin, as shown in Fig. 1.

Compound **2** showed IR and UV spectra similar to those of **1**, indicating that **2** was a lasiodiplodin derivative of **1**. In the  $^1\text{H}$  and  $^{13}\text{C}$ -NMR spectra (Tables 1 and 2), new signals were assigned to one *trans* double bond [ $\delta_{\text{H}}$  5.72–5.80 (m, H-9), 6.84 (1H, d,  $J = 15.2$  Hz, H-10);  $\delta_{\text{C}}$  125.9 (C-9), 136.7 (C-10)]. For comparative purposes, **2** was hydrogenated using palladium on carbon (Pd/C). The  $^1\text{H}$  and  $^{13}\text{C}$  NMR spectra of hydrogenated **2** corresponded to those of **1**. Based on these results, the structure of **2** was assigned to (*3S,7R*)-9-etheno-7-hydroxy-13-*O*-methyl-*de*-*O*-methylsiasiodiplodin (Fig. 1).

The molecular formula of **3** was determined to be  $\text{C}_{16}\text{H}_{20}\text{O}_5$  by HRESITOFMS. Comparisons of 1D and 2D NMR and the HRESITOFMS data for **3** against values in the literature allowed **3** to be identified as 7-oxo-*de*-*O*-methylsiasiodiplodin, which was previously isolated from the mycelium extracts of a brown alga endophytic fungus (No. ZZP36) obtained from the South China Sea (Yang et al., 2006). However, the optical rotation of **3** ( $[\alpha]_{\text{D}} = -36.7$ ,  $c$  0.02,  $\text{CHCl}_3$ ) was opposite in sign to that previously reported for the natural compound ( $[\alpha]_{\text{D}} = +38.89$ ,  $c$  0.02,  $\text{CHCl}_3$ ), indicating that **3** must be the *S* enantiomer of (*3R*)-7-oxo-*de*-*O*-methylsiasiodiplodin (Fig. 1).

The molecular formula of **4** was established as  $\text{C}_{13}\text{H}_{16}\text{O}_6$ , based on the HRESITOFMS measurement, which was 14 mass units less than that for **5** (Fig. S25) (Sato et al., 2021). The difference between **4** and **5**

was clearly that the  $\text{OCH}_3$  ( $\delta_{\text{C}}$  3.68, Table S1) found in **5** was missing from the  $^1\text{H}$  NMR spectrum of **4**, which suggested that **4** was a methylated derivative of **5**. During our purification procedure, methanol extraction was performed; therefore, **4** could be an artifact of **5**.

Four known compounds were identified: 3-(2-ethoxycarbonyl-3,5-dihydroxyphenyl) propionic acid (**5**), (*S*)-ethyl 2,4-dihydroxy-6-(8-hydroxynonyl) benzoate (**6**), ethyl 2,4-dihydroxy-6-(8-oxononyl) benzoate (**7**), and 3-(2-ethoxycarbonyl-3,5-dihydroxyphenyl) propionic acid (**8**) (Fig. S25). In this study, all compounds were subjected to the plant regulatory assay utilizing *L. sativa* and *D. ciliaris* (Fig. 5 for **1–3** and Fig. S19 for **4–8**), in which the positive control, 2,4-dichlorophenoxyacetic acid, significantly inhibited the growth of *L. sativa* and *D. ciliaris*. Compound **1** showed the most prominent inhibitory effects among the tested compounds, inhibiting the root growth of *D. ciliaris*. Compound **2**, which possessed a common skeleton as **1**, with a double bond and a hydroxyl group at C-7, did not present similar phytotoxicity as **1**, suggesting that the conformational freedom of the macrocyclic ring appears to be an important structural feature for phytotoxicity. Compounds **6**, **7**, and **8** enhanced elongation activity toward the *L. sativa* root, similar to our previous report (Fig. S19) (Sato et al., 2021). In our previous report (Sato et al., 2021), **8** demonstrated a phytotoxic effect on the leaves, which presented visible yellow lesions at 100 ppm. Therefore, compounds **1–7** were evaluated for their phytotoxic activities against *D. ciliaris* leaves. Compounds **6** and **7** caused yellow lesions on the leaves (Fig. 6). The opening of the macrolactone ring appears to play a significant role in phytotoxic activity.

## 2. Conclusion

In conclusion, eight metabolites were isolated from the culture of *L. theobromae* and, three of them were assigned as newly identified compounds: (*3S,7R*)-7-hydroxy-13-*O*-methyl-*de*-*O*-methylsiasiodiplodin (**1**), (*3S,7R*)-9-etheno-7-hydroxy-13-*O*-methyl-*de*-*O*-methylsiasiodiplodin (**2**), and (*3S*)-7-oxo-*de*-*O*-methylsiasiodiplodin (**3**).

Lasioidiplodins, widely distributed fungal metabolites, have been identified in various plants and fungi, and exhibit several bioactive properties (Bang and Shim, 2020), including antimicrobial (Yang et al., 2006), phytotoxic (Sato et al., 2021), potato micro-tuber inducing (Qing et al., 2000), antioxidant (Ekuadzi et al., 2014), and cytotoxic (Shen et al., 2015) activities. In this study, compound **1** showed phytotoxic activities against *L. sativa* and *D. ciliaris*. Although compounds **6** and **7** demonstrated an elongation effect on the roots, they caused the development of visible yellow lesions at 100 ppm. These activities of **1**, **6**, and **7** are sufficient to warrant further study of their modes of action and, perhaps, their roles in chemical ecology, including allelopathy.

## 3. Materials and methods

### 3.1. General experimental procedures

Optical rotations were measured using a Horiba SEPA-300 polarimeter (Horiba, Japan). IR and UV spectra were recorded with

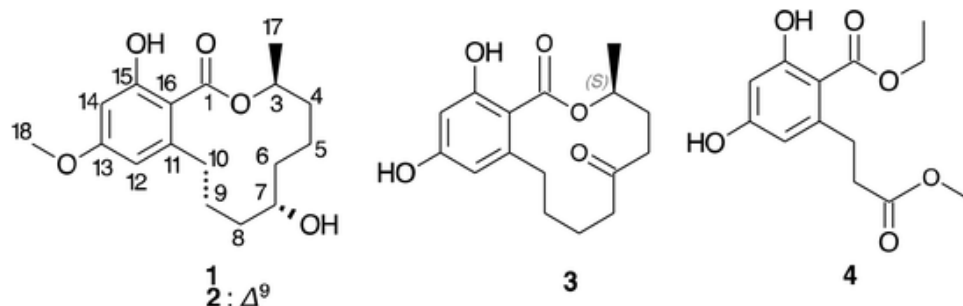


Fig. 1. Chemical structures of 1–4.

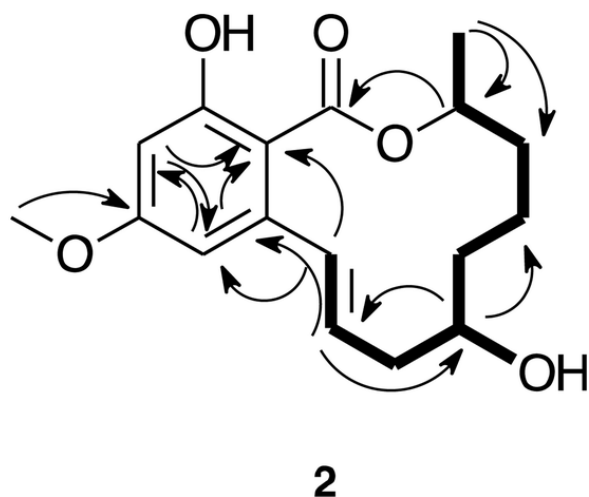
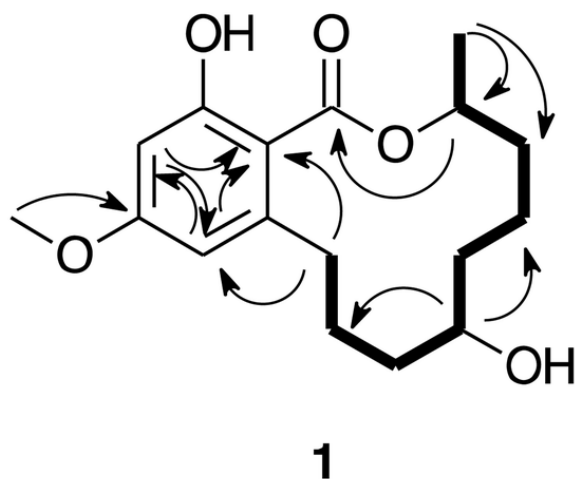


Fig. 2.  $^1\text{H}, ^1\text{H}$  COSY (bold lines) and selected HMBC (arrows) correlations of **1** and **2**.

Horiba FT710 (Horiba, Japan) and Shimadzu UV-1800 spectrometer (Shimadzu, Japan), respectively. Mass spectra were obtained with a Synapt G2 (Water Corporation, USA) and JEOL HX110 mass spectrometer (JEOL, Japan). NMR data were recorded on JEOL ECZ-600 spectrometer (JEOL, Japan) at 600 MHz for  $^1\text{H}$  and 150 MHz for  $^{13}\text{C}$ . Chemical shift are given on a  $\delta$  (ppm) scale with TMS as an internal standard.  $^1\text{H}$ ,  $^{13}\text{C}$ , DEPT, COSY, HMQC, and HMBC spectra were recorded using standard JEOL pulse sequences. Column chromatography were conducted on silica gel 60 (Kanto Chemical Co., Inc., Japan) and ODS (Fuji Silysia, Japan). Flash chromatography were conducted using Büchi Flash Chromatography C-601 (Büchi, Switzerland) and packed column Biotage® SNAP Ultra (Biotage, Sweden) 10 g (25  $\mu\text{m}$ ). HPLC separations were carried out using Shimadzu LC-20AT and UV-vis detector SPD-20A (Shimadzu, Japan) on reverse phase-high performance liquid chromatography (RP-HPLC) packed column C-18 UG80 (Shiseido, Japan). Thin layer chromatography (TLC) were carried out on precoated silica gel 60 F<sub>254</sub> plates (Merck, Germany), and spot were detected by spraying with 1% vanillin in  $\text{H}_2\text{SO}_4$  followed by heating, or by UV irradiation.

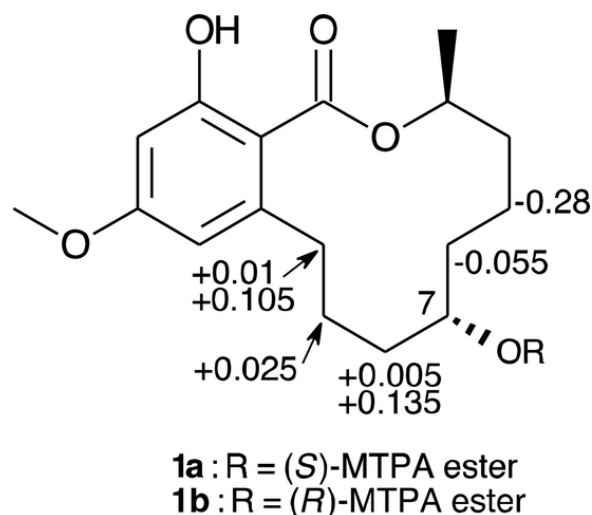


Fig. 3.  $\Delta\delta = \delta_S - \delta_R$  values in ppm obtained from the MTPA esters (**1a** and **1b**).

### 3.2. Fungal material and fermentation

The fungal strain GI-1005 was isolated from inner tissue of a branch (*Rhizopora mucronata*) collected in the Santolo beach area (southern latitude  $7^\circ 65' 00''$ , east longitude  $107^\circ 68' 76''$ ), Garut, West Java, Indonesia. This strain was identified as *Lasiodiplodia theobromae* using DNA analysis of the 18S rRNA regions. This fungus was deposited at our laboratory in the Faculty of Agriculture, Yamagata University. *L. theobromae* was cultivated on sterilized brown rice (120 g in five 1 L flasks) at  $25^\circ\text{C}$  for four weeks.

### 3.3. Fermentation, extraction, and isolation

To prepare the seed culture, the strain (GI-1005) was cultured on potato dextrose agar (PDA) at  $25^\circ\text{C}$  for 6 days. The agar plugs were cut into small pieces ( $1\text{cm}^2$ ) and then inoculated into 10 Erlenmeyer flasks (1 L) containing 120 g of rice and 120 mL of distilled water, which were previously sterilized by autoclaving. All flasks were incubated at  $25^\circ\text{C}$  for 30 days. The culture was extracted with methanol, and the methanol was removed under reduced pressure to yield a crude extract (17.5 g). The crude extract was partitioned between ethyl acetate and water to obtain the ethyl acetate-soluble fraction (5.2 g). This part was separated by column chromatography on silica gel (*n*-hexane – EtOAc, 100:0 to 0:100, and EtOAc-MeOH, 50:50, and 0:100) to give 13 fractions (Fr. 1-1 to Fr. 1-13). Fr. 1-7 (2.37 g, 60 % EtOAc) was separated using silica gel column chromatography ( $\text{CHCl}_3$ -EtOAc, 100:0 to 0:100, and EtOAc-MeOH, 50:50 and 0:100) to obtain 13 fractions (Fr. 2-1 to Fr. 2-13). Fr. 2-8 (1.44 g, 70 % EtOAc) was further separated on an ODS column (MeOH- $\text{H}_2\text{O}$ , 100:0 to 0:100) to yield 11 fractions (Fr. 3.1 to Fr. 3.11). Fr. 3-7 (30.6 mg, 60 % MeOH) was further separated using silica gel flash column chromatography (*n*-hexane- EtOAc, 70:30) to afford 20 fractions (Fr. 3-7 -1 to Fr. 3-7 -20). Fr. 3-7 -19 (10.4 mg) was purified by repeated semipreparative HPLC (MeOH- $\text{H}_2\text{O}$ , 75:25) to yield compound **3** (7.0 mg). Fr. 3-9 (45.2 mg, 80 % MeOH) was further separated using silica gel flash column chromatography (*n*-hexane-EtOAc, 70:30) to afford the crude fractions including compounds **1** and **2**. These fractions (23 mg) were further purified by repeated semipreparative HPLC (MeOH- $\text{H}_2\text{O}$ , 75:25) to yield compounds **1** (7.0 mg), and **2** (3.4 mg).

#### 3.3.1. (3S,7R)-7-hydroxy-13-O-methyl-de-O-methyl-lasiodiplodin (**1**)

White amorphous powder;  $[\alpha]_D^{20}$  -29.1 (c 0.4, MeOH); UV (MeOH)  $\lambda_{\text{max}}$  (log  $\epsilon$ ) 217 (3.64), 264 (3.38), 303 (3.00) nm; ECD (MeOH)  $\lambda_{\text{max}}$

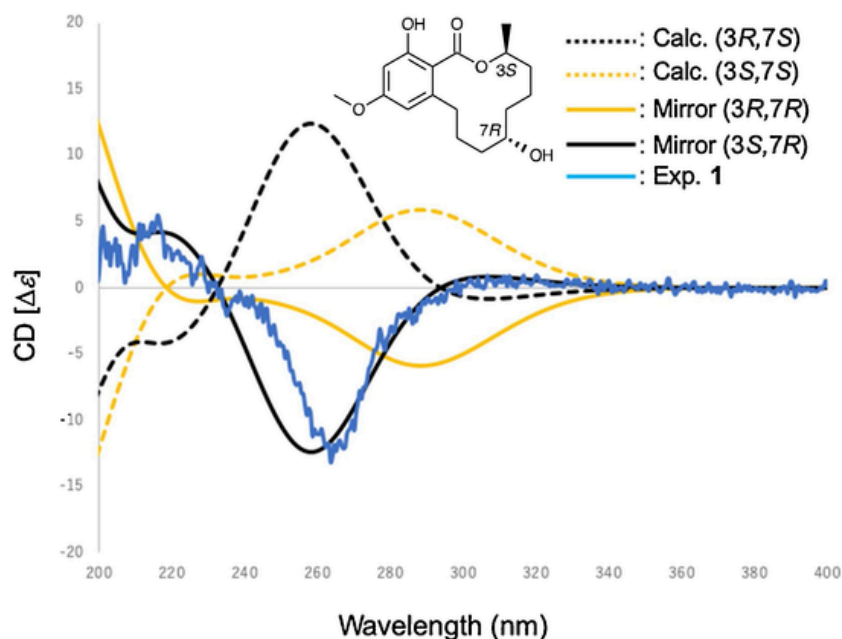


Fig. 4. Calculated and experimental ECD spectra of **1**.

Table 2

<sup>1</sup>H-NMR NMR Data (600 MHz in CDCl<sub>3</sub>, and  $\delta$  in ppm and  $J$  in Hz) for Compounds **1–3**.

No.	1	2	3
3	5.09–5.16 (m)	5.25–5.31 (m)	5.28–5.34 (m)
4	1.44–1.84*	1.61–1.77 (m)	2.16–2.27 (m)
5	1.44–1.84*	1.42–1.55 (m)	2.40–2.49 (m) 2.67–2.78 (m)
6	1.44–1.84*	1.55–1.70(m)	
7	3.89–3.96 (m)	3.91–3.96 (m)	2.50–2.57 (m) 2.70–2.80 (m)
8	1.25–1.32 (m) 1.91–2.10 (m)	2.42–2.55 (m)	1.64–1.72 (m) 1.80–1.87 (m)
9	1.47–1.84 (m)	5.72–5.80 (m)	1.35–1.44 (m) 1.53–1.61 (m)
10	2.13–2.20 (m) 3.63–3.71 (m)	6.84 d (15.2)	2.41–2.49 (m) 3.01–3.09 (m)
12	6.27 d (2.7)	6.36 d (2.4)	6.17 d (3.0)
14	6.32 d (2.7)	6.34 d (2.4)	6.24 d (3.0)
17	1.34 d (6.2)	1.36 d (6.0)	1.38 d (6.0)
18	3.74 s	3.79 s	
OH	11.99 s	10.76 s	11.96 s

\* Overlapped signals.

( $\Delta\epsilon$ ) 215 (4.7), 264 (-13.5) nm; IR (KBr)  $\nu_{\max}$  3339, 2930, 1642, 1614, 1580, 1350, 1297, 1254, 1207, 1158, 1043 cm<sup>-1</sup>; <sup>1</sup>H-NMR (600 MHz, CDCl<sub>3</sub>) and <sup>13</sup>C-NMR (150 MHz, CDCl<sub>3</sub>) data, see Tables 1 and 2; HRESITOFMS (positive ion mode)  $m/z$  331.1515 ([M + Na]<sup>+</sup>, calcd. for C<sub>17</sub>H<sub>24</sub>O<sub>5</sub>Na, 331.1522).

### 3.3.2. (3*S*,7*R*)-9-etheno-7-hydroxy-13-*O*-methyl-*de*-*O*-methylasiadiplodin (**2**)

White amorphous powder; [ $\alpha$ ]<sub>D</sub><sup>20</sup> -131.8 (c 0.2, MeOH); UV (MeOH)  $\lambda_{\max}$  (log  $\epsilon$ ) 227 (3.58), 267 (3.27), 306 (2.96) nm; IR (KBr)  $\nu_{\max}$  3311, 2939, 1652, 1614, 1574, 1506, 1356, 1254, 1204, 1161, 1036 cm<sup>-1</sup>; <sup>1</sup>H-NMR (600 MHz, CDCl<sub>3</sub>) and <sup>13</sup>C-NMR (150 MHz, CDCl<sub>3</sub>) data, see Tables 1 and 2; HRESITOFMS (positive ion mode)  $m/z$  329.1359 ([M + Na]<sup>+</sup>, calcd. for C<sub>17</sub>H<sub>22</sub>O<sub>5</sub>Na, 329.1365).

### 3.3.3. (3*S*)-7-oxo-*de*-*O*-methylasiadiplodin (**3**)

White amorphous powder; [ $\alpha$ ]<sub>D</sub><sup>20</sup> -36.7 (c 0.02, CHCl<sub>3</sub>); UV (MeOH)  $\lambda_{\max}$  (log  $\epsilon$ ) 211 (3.82), 266 (3.63), 303 (3.25) nm; IR (KBr)  $\nu_{\max}$  3330, 2948, 2865, 1695, 1639, 1446, 1310, 1257, 1204, 1170, 1092, 1012 cm<sup>-1</sup>; <sup>1</sup>H-NMR (600 MHz, CDCl<sub>3</sub>) and <sup>13</sup>C-NMR (150 MHz, CDCl<sub>3</sub>) data, see Tables 1 and 2; HRESITOFMS (positive ion mode)  $m/z$  315.1208, C<sub>16</sub>H<sub>20</sub>O<sub>5</sub>Na, ([M + Na]<sup>+</sup>, calcd. for 315.1209).

### 3.4. Preparation of MTPA ester derivatives (**1a** and **1b**) from **1**

To **1** (1.0 mg) in dry pyridine was added (*R*)-(-)-MTPACl (10  $\mu$ L), then the mixture was stirred at room temperature for 24 h. Purification by column chromatography has been done on silica gel (*n*-hexane: EtOAc) to afford the (*S*)-MTPA ester (**1a**, 0.9 mg). Compound **1** (1.0 mg) was treated with (*S*)-(+)-MTPACl (10  $\mu$ L) in the same procedure to afford the (*R*)-MTPA ester (**1b**, 0.9 mg).

**1a**: HRESITOFMS (positive ion mode)  $m/z$  547.1960 [M + Na]<sup>+</sup> (calcd. for C<sub>27</sub>H<sub>31</sub>F<sub>3</sub>O<sub>7</sub>Na 547.1918); <sup>1</sup>H (600 MHz, CDCl<sub>3</sub>)  $\delta_{\text{H}}$  0.85–0.88 (m, H-8), 1.36 (1H, d,  $J$  = 5.4 Hz, H-17), 1.42–1.67 (m, H-4, 5, 6) 1.74–1.77 (m, H-9), 2.09–2.15 (m, H-8) 2.15–2.16 (m, H-10), 3.53 (3H, OMe of MTPA), 3.63–3.67 (m, H-10), 3.79, (3H, s, 10-OMe), 5.19–5.22 (m, H-3), 5.32–5.37 (m, H-7), 6.26 (1H, d,  $J$  = 2.4 Hz, H-12), 6.34 (1H, d,  $J$  = 3.0 Hz, H-14), 7.34–7.39 (3H, m, Ph of MTPA), 7.48–7.51 (2H, m, Ph of MTPA), 12.08 (1H, s 15-OH).

**1b**: HRESITOFMS (positive ion mode)  $m/z$  547.1958 [M + Na]<sup>+</sup> (calcd. for C<sub>27</sub>H<sub>31</sub>F<sub>3</sub>O<sub>7</sub>Na 547.1918); <sup>1</sup>H (600 MHz, CDCl<sub>3</sub>)  $\delta_{\text{H}}$  0.84–0.88 (m, H-8), 1.04 (1H, d,  $J$  = 6.0 Hz, H-17), 1.24–1.41 (m, H-4) 1.59–1.61 (m, H-5), 1.69–1.77 (m, H-9), 1.81–1.84 (m, H-6), 1.96–2.01 (m, H-8), 2.04–2.06 (m, H-10), 3.54 (3H, OMe of MTPA), 3.62–3.66 (m, H-10), 3.79 (3H, s, 18-OMe), 5.07–5.12 (m, H-3), 5.28–5.36 (m, H-7), 6.57 (1H, d,  $J$  = 1.2 Hz, H-12), 6.65 (1H, d,  $J$  = 1.2 Hz, H-14), 7.42–7.45 (3H, m, Ph of MTPA), 7.54–7.57 (2H, m, Ph of MTPA), 12.01 (1H, s, 15-OH).

### 3.5. Seedling growth assays

Two plants, *Digitaria ciliaris* and *Lactuca sativa*, were used as receiver plants for testing the phytotoxic activity of the isolated compounds. Seeds of *D. ciliaris* and *L. sativa* were surface sterilized with a flowing tap water before use. Isolated compounds were dissolved in methanol.

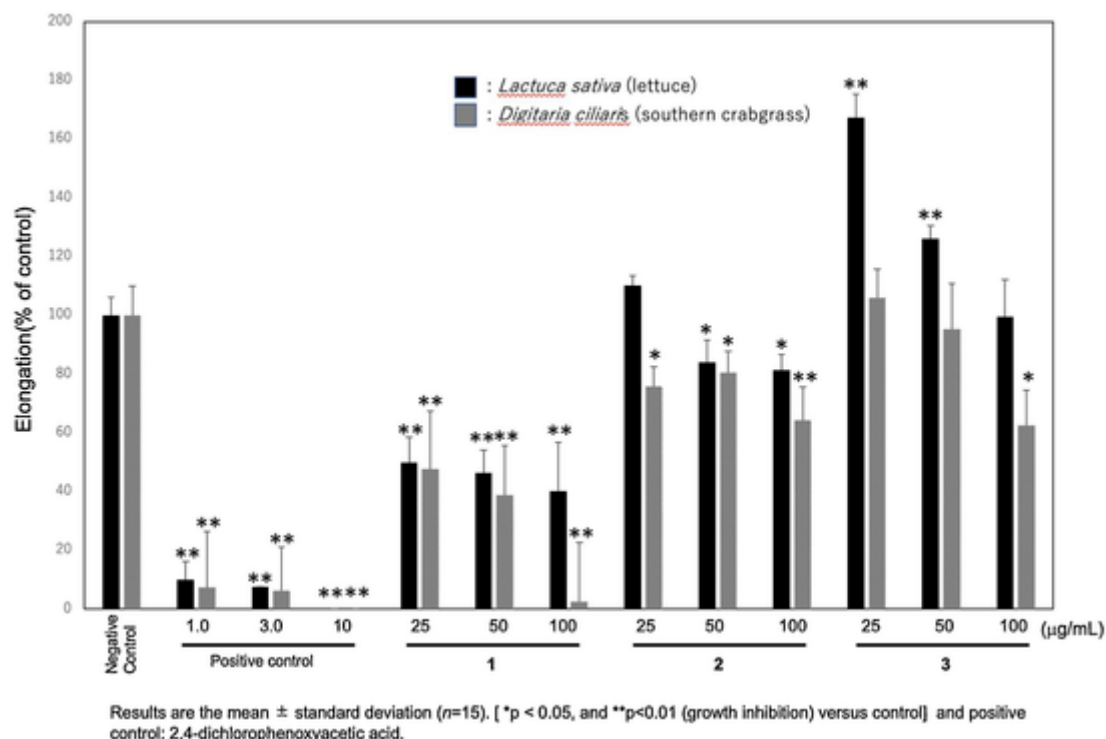


Fig. 5. Effects of 1 - 3 on the seedling growth of *Lactuca sativa* (lettuce) and *Digitaria ciliaris* (southern crabgrass) ( $\mu\text{g/mL}$ ).

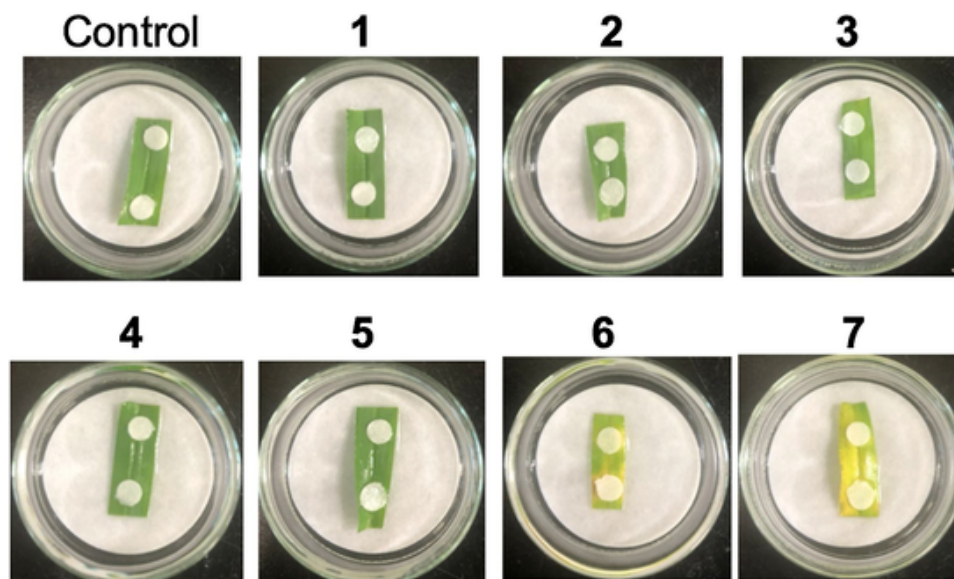


Fig. 6. Phytotoxic effects on the leaves of *Digitaria ciliaris* by 1 - 7 (3 days).

The MeOH solutions (25, 50 and 100  $\mu\text{L}$ ) containing a sample at the definite concentration (1000  $\mu\text{g/mL}$ ) were poured on to each piece of filter paper in Petri dishes (4.0 cm diameter). After complete evaporation of methanol, distilled water (1 mL) was added to each petri dish followed by addition of 15 seeds. All petri dishes were stored in the dark at 25  $^{\circ}\text{C}$ . Seedlings were allowed to grow for 7 (for *L. sativa*) or 10 (for *D. ciliaris*) days before shoot and root length were measured. Three replicates were made for each treatment ( $n = 15$ ).

### 3.6. Phytotoxicity assay

Fresh *Digitaria ciliaris* leaves were washed three times with sterilized water. The leaves were cut into 1.0  $\times$  3.0 cm rectangle with scissors

and placed in a sterile glass dish. A 1 mg amount of test compound was dissolved in MeOH aqueous solution contains 90 % (v/v) water to produce a 1.0 mg/0.1 mL test solution. Two filter piece discs (8 mm diameter) were placed on the leaves, and then 10  $\mu\text{L}$  of MeOH aqueous solution or test solution was added to each disc. The effect was recorded after 3 and 5 days of observation.

### 3.7. ECD calculations

In order to clarify the absolute configurations of 1, computational methods were utilized. The DFT and TDDFT calculations were carried out in the gas phase with Gaussian 09 software (Frisch et al., 2009). The conformational analysis was initially performed using the GMMX

program (Halgren et al., 1996) with the MMFF94 force field. The selected conformer was optimized at B3LYP/6–31 G(d) using DFT. The ECD calculations were conducted using the TDDFT method for 30 excited states at the B3LYP/6–311 G (d) level in the gas phase. The CD spectra were generated by the program SpecDis using a Gaussian band shape with 0.3 eV.

### Declaration of Competing Interest

The authors report no declarations of interest.

### Acknowledgements

The authors thank Prof. Hiroyuki Konno and Prof. Takako Aboshi in Yamagata University for CD and MS experimental supports, respectively. This work was partly supported by JSPS MEXT KAKENHI Grant Number JP19K05709 (Y. S) and the author (U. S) was also supported by World Class Professor Grant Number T/83/D2.3/KK.04.05/2019, Indonesia).

### Appendix A. Supplementary data

Supplementary material related to this article can be found, in the online version, at doi:<https://doi.org/10.1016/j.phytol.2021.05.003>.

### References

- Bang, S., Shim, S.H., 2020. Beta resorcylic acid lactones (RALs) from fungi: chemistry, biology, and biosynthesis. *Arch. Pharm. Res.* 43, 1093–1113.
- Bastias, D.A., Martínez-Ghersa, A., Ballaré, C.L., Gundel, P.E., 2017. Epichloë fungal endophytes and plant defenses: not just alkaloids. *Trends Plant Sci.* 22, 939–948.
- Ekuadzi, E., Dickson, R.A., Fleischer, T.C., Amponsah, I.K., Pistorius, D., Oberer, L., 2014. Chemical constituents from *Gouania longipetala* and *Glyphaea brevis*. *Nat. Prod. Res.* 28, 1210–1213.
- Hiruma, K., Kobae, Y., Toju, H., 2018. Beneficial associations between Brassicaceae plants and fungal endophytes under nutrient-limiting conditions: evolutionary origins and host–symbiont molecular mechanisms. *Curr. Opin. Plant Biol.* 44, 145–154.
- Martinez-Klimova, E., Rodríguez-Peña, K., Sánchez, S., 2017. Endophytes as sources of antibiotics. *Biochem. Pharmacol.* 134, 1–17.
- Qing, Y., Maki, A., Hidayuki, M., Teruhiko, Y., 2000. Potato micro-tuber inducing hydroxylasiodiplodins from *Lasiodiplodia theobromae*. *Phytochemistry* 54, 489–494.
- Sato, S., Sofian, F.F., Suehiro, W., Harneti, D., Maharani, R., Supratman, U., Abdullah, F., Salam, S., Koseki, T., Shiono, Y., 2021.  $\beta$ -resorcylic acid derivatives, with their phytotoxic activities, from the endophytic fungus *lasiodiplodia theobromae* in the mangrove plant *Xylocarpus granatum*. *Chem. Biodivers.* 18. <https://doi.org/10.1002/cbdv.202000928>.
- Segaran, G., Sathia velu, M., 2019. Fungal endophytes: a potent biocontrol agent and a bioactive metabolites reservoir. *Biocatal. Agric. Biotechnol.* 21. <https://doi.org/10.1016/j.cbab.2019.101284>.
- Shen, W., Mao, H., Huang, Q., Dong, J., 2015. Benzenediol lactones: a class of fungal metabolites with diverse structural features and biological activities. *Eur. J. Med. Chem.* 97, 747–777.
- Yang, R.-Y., Li, C.-Y., Lin, Y.-C., Peng, G.-T., She, Z.-G., Zhou, S.-N., 2006. Lactones from a brown alga endophytic fungus (No. ZZ36) from the South China Sea and their antimicrobial activities. *Bioorg. Med. Chem. Lett.* 16, 4205–4208.